ATLAS-BASED MOTION CORRECTION FOR ON-LINE MR TEMPERATURE MAPPING

B. Denis de Senneville[1,2,3]*, B. Quesson*[2]*, P. Desbarats*[3]*, R. Salomir*[4]*, J. Palussière*[5]*, C. T. W. Moonen*[1]

[1] IMF, ERT CNRS/Université Bordeaux 2 - 146, rue Léo Saignat, F-33076 Bordeaux
[2] Image Guided Therapy SA - 2, allée du doyen George Brus, F-33600 Pessac
[3] LaBRI, UMR 5800 CNRS/Université Bordeaux 1 - 351, cours de la Libération, F-33405 Talence
[4] U386 INSERM, France
[5] Institut Bergonié, France
{baudouin,quesson,desbarats,salomir,moonen}@imf.u-bordeaux2.fr

ABSTRACT

Magnetic Resonance (MR) temperature mapping can be used to monitor temperature changes in minimally invasive thermal therapies during the procedure. However, organs displacements due to physiological activity (heart and respiration) may induce important artifacts on apparent temperature maps. This paper presents a new method for motion quantification and correction in such MR images, in order to improve the precision of temperature estimation using the proton resonance frequency (PRF) shift. The PRF shift technique gives an estimate of the relative temperature variation, comparing contrast between dynamically acquired images and a reference data sets. The correction method described in this paper consists of two steps : a motion atlas is initially computed in a preparation phase; during the intervention, the appropriate reference image is chosen from the atlas, allowing correct computation of the temperature map despite tissue motion. This method can be applied to any type of image sequences and is not restricted to MR images.

1. INTRODUCTION

Local hyperthermia can be used for a wide variety of medical interventions such as tumor ablation [1] [2], treatment of heart arrhythmias [3], local drug delivery with thermosensitive microcarriers [4] [5] and control of gene therapy using heat-sensitive promoters [6]. MRI is the only imaging technique that can provide both anatomical and on line quantitative thermometry information simultaneously. The main principle of MRI is based on the detection of magnetic properties of the protons contained in the water molecules of the body [7]. The MR imaging system associates each voxel of the observed region of interest with a complex number $Me^{i\phi}$, where M is the magnitude and ϕ the phase of the macroscopic magnetization. This magnetization rotates in space in each pixel and can be represented by a magnitude image M and a phase image ϕ (as shown in Fig. 1.A and Fig. 1.C).

The rotation frequency of the magnetization varies linearly with temperature [8]. Temperature maps can then be calculated from two phase images obtained before (cf Fig. 1.C) and during the heating procedure (1.D) as shown in Fig. 1.E.

Unfortunately, the acquisition procedure of MRI temperature is prone to specific artifacts [9]. This technique is highly sensitive to motion artifacts (patient motion, respiration, cardiac activity) and to dynamic changes of the local magnetic field. The sensitivity of this method has limited its application to organs with little mobility or easily restrained like muscle, breasts and the prostate.

The most simple technique to reduce respiration artifacts is to synchronize the acquisition of the images to a stable period of the respiratory cycle, usually at the end of expiration. On line evolution of the respiration can be monitored by using a pressure sensor positioned on the abdomen of the subject. The major drawback of this method is that the temporal resolution depends on the respiration frequency and a limited set of images (up to five adjacent slices) can be acquired during a respiratory cycle (approximatively 5 seconds for humans). However, irregular and/or deep respiration movements can induce erroneous temperature mapping (up to 20^oC).

Our approach consists of 1) performing rapid acquisition (acquisition time per image faster than typical motion period) of MR images without synchronization methods, 2) applying specific image processing techniques to estimate motion on anatomical images and, 3) correcting corresponding phase images to remove temperature artifacts. As temperature evolution needs to be visualized during the procedure, corrections must be performed on line (within the delay between two successive acquisitions). A compromise on the acquisition parameters has to be performed to obtain a sufficient SNR (Signal to Noise Ratio), while shortening acquisition duration. In the case of respiratory motion, typical acquisition duration of 400ms for one slice was found to be a reasonable value to obtain a sufficient SNR and to avoid intra-scan motion artifacts.

A number of motion correction techniques have already been developed for functional MRI but all the algorithm are based on rigid transformations. Unfortunately, this assumption cannot be applied on the abdomen, particularly for liver and kidney. In addition, all these algorithms are used in post-treatment but not on line.

2. METHOD DESCRIPTION

In practice, under on line conditions, it is hardly feasible to acquire isotropic 3D temperature maps on mobile organs, due to technical limitations of MR acquisition sequences. Our approach is to estimate organs displacements in the 2D images generated from objects that are moving in 3D space.

Fig. 1 shows typical coronal magnitude and phase images obtained on a healthy volunteer at different times of the respiratory cycle. The spatial resolution of those images is 128×128 pixels and the pixel size is $2,5 \times 2,5mm$.

0-7803-8554-3/04/$20.00 ©2004 IEEE.

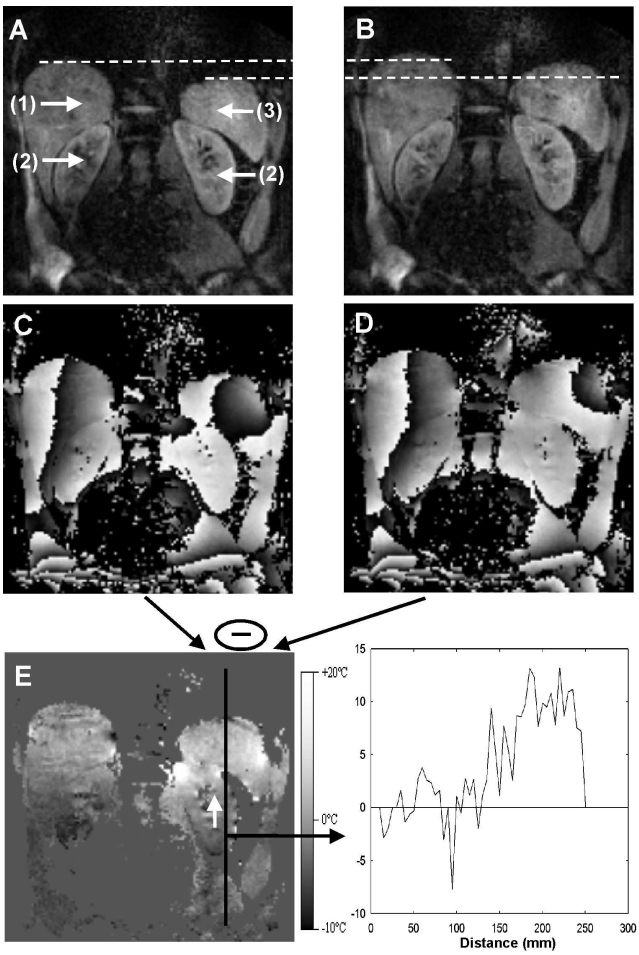

Fig. 1. MR anatomical and phase images obtained at different times on a free breathing volunteer. Magnitude and phase image acquired at the beginning of the expiration (resp A and C), and at the end of the expiration (resp B and D) - E : temperature map proportional to the difference between C and D - F : temperature profile in the direction of the motion in a selected line reported on E.

Vertical displacement of the liver (1), kidneys (2) and the spleen (3) can be observed (horizontal white dashed lines). Temperature map calculated from the difference of phase images is affected, as shown on grey levels differences on image E. In this example, apparent temperature ranged between -8^oC to 12^oC (as shown on the profile), whereas no effective heating of the tissues was induced.

Fig. 2 presents the temporal evolution of the temperature measured on a single pixel located on the left kidney of the subject (white arrow reported on Fig. 1.E). Important oscillations (amplitude in the range of 15^oC) of the apparent temperature dramatically hamper the precision of quantitative MR temperature mapping.

The main idea of our method is to construct a motion atlas based on images obtained during a pre-treatment phase (no hyperthermia) using the same sequence as for the intervention. For that

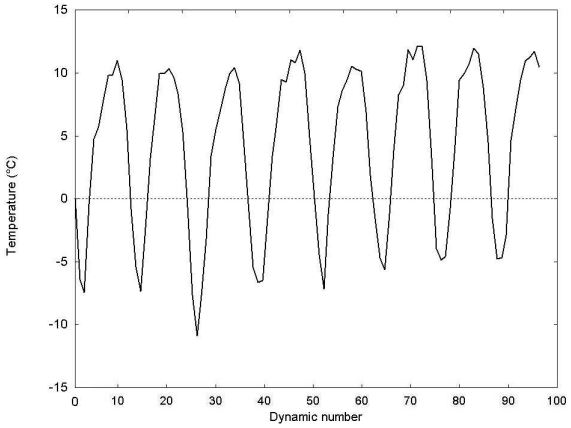

Fig. 2. Temporal evolution of the temperature on a single pixel located on the left kidney of the subject (white arrow reported on Fig. 1.E)

purpose, one hundred 128x128 images (400ms per image) were acquired to allow a precise sampling of the respiratory cycle. During this pre-treatment phase, an apparent motion field can be calculated for each magnitude image. For each position, this motion field is stored with the corresponding phase image to create an atlas of correction data set.

The reference image set (magnitude and phase) is chosen to be the first one in the temporal serie. Each time a new data set is available, corresponding temperature map is processed from phase difference and the temperature standard deviation is calculated. If this value exceeds a preset threshold (typical value is 2^oC) defined by the radiologist, the image data set is considered as artifacted and needs to be corrected for motion.

During the intervention, organs displacements in an artifacted image can then be estimated and compared to the reference motion values stored in the atlas. The nearest motion field in the atlas is selected, and the corresponding phase image is used as reference for the temperature computation.

3. MOTION ESTIMATION TECHNIQUES

Our approach consists of using image processing techniques to detect organ displacements on the anatomic images on line. The objective is to relate the coordinate of each part of tissue in the image we want to register with the corresponding tissue in the reference image.

Motion estimation field computed from image sequences has a growing interest because of the considerable number of applications (biomedical, material study, meteorology, video compression...).

If $I_{ref}(X)$ is a reference image and $I(X')$ the image to register, where X and $X' \epsilon \Re^n$ ($n = 2$ for the 2D image registration problem). Registering $I(X)$ is equivalent to estimating the coordinate transformation V that minimize :

$$\min M\left(I(X), I_{ref}(V(X'))\right)$$

where M is any matching criteria defined on the images.

3.1. Choice of motion estimation method

The most restrictive registration techniques are methods using parameterized models because the algorithm calculates a global transformation. These methods are based on a parameterized model of motion [10]. Identification of the displacement is done by optimizing model parameters (for example, six parameters in an affine model). The choice of the model requires to know the nature of the movement to obtain reliable results.

The "Block-matching" technique is used in the video compression (MPEG format). The image to be registered is divided in blocks and the translation of each block is estimated in a research window [11]. It is supposed that the motion in the image is constant in a region. This technique is then less restrictive because it estimates and corrects local motion. Therefore there is no limitation in the transformation that can be applied to the original image.

Optical flow computation consists in extracting a velocity field from an image sequence assuming that intensity is conserved during displacement. As can be seen on Fig. 1. A and B, this assumption is verified in the present case. Many methods can provide an estimation of the optical flow such as correlation methods (establishing a correspondence between two images by localization of invariant markers such as pixels where the intensity variations is high [12], [13]) and differential methods.

The choice of the registration method depends on the part of the body observed. In our case, all organs undergo individual motion indicating that a very permissive method is preferable. We decided to use the differential approach established by Horn and Schunck [14] because there is no limitation with the transformation that can be applied to the original image. However, this technique requires an intensity conservation between compared images and a regular displacement between adjacent pixels.

Mathematically, intensity conservation implies that two values u and v exist and verify the following expression :

$$I(x, y, t) = I(x + u\delta t, y + v\delta t, t + \delta t)$$

A Taylor model of order 1 gives (I_x, I_y, I_t are the partial derivative of order 1) :

$$I(x, y, t) = I(x, y, t) + I_x u\delta t + I_y v\delta t + I_t \delta t + \epsilon$$

The estimation process consists then in minimizing :

$$I_x u + I_y v + I_t$$

The second condition of this method is that motion field is regular in the image. This constraint requires that u and v should have similar values for adjacent pixels. Mathematically this constraint can be expressed with the following minimization :

$$\int\int \left(u_x^2 + u_y^2 + v_x^2 + v_y^2\right) dxdy$$

Finally, combination of the two constraints results in numerical minimization of the following expression :

$$I_x u + I_y v + I_t + \alpha^2 \left[u_x^2 + u_y^2 + v_x^2 + v_y^2\right]$$

where α^2 is a user defined weighting factor.

This minimization problem can be numerically solved with an iterative scheme like Gauss-Seidel.

This algorithm has been implemented in C++ and tested for each images of the pretreatment phase and during the intervention.

3.2. Motion field atlas computation

Each image set detected as artifacted from the temperature standard deviation computation is processed as follow. First, organs displacements are estimated from the magnitude images using the method described above. Motion vectors are then described by two images representing horizontal and vertical displacements, respectively. This new data set is stored in the RAM with the associated phase image.

3.3. Dynamic selection of analog displacement from the atlas

During the intervention, each new data set is tested with the same method as for atlas computation (threshold on the standard deviation on the temperature), excluding the heated region. Motion field of each artifacted data set is extracted in a similar way and compared to the atlas. Euclidian distance between current motion field and each motion field of the atlas is calculated and stored in a list. Phase image in the atlas corresponding to the smallest euclidian distance in this list is selected as a reference for temperature calculation.

4. RESULTS AND DISCUSSION

The implemented algorithm for image registration required 250ms of computation time on an Athlon 2800MHz with 512Mo of RAM, demonstrating that temperature correction can be performed on line under these experimental conditions.

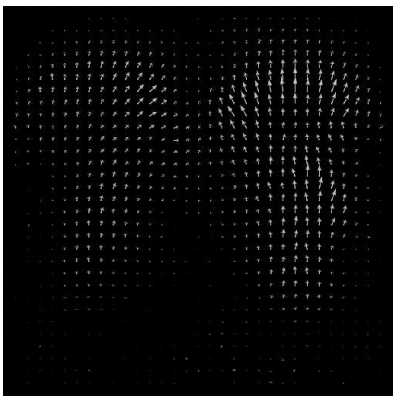

Fig. 3. Motion field estimation with Horn & Schunck method

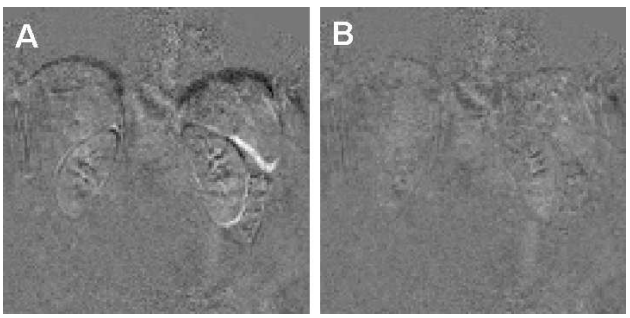

Fig. 4. Substraction of reference image with motion corrupted image (A) and motion corrected image (B)

Fig. 3 shows the motion field resulting from computation of image A and B of Fig. 1 with the Horn and Schunck method. Displacements direction is mainly vertical, as expected, with a higher value for the liver as compared to the kidneys.

Fig. 4 compares magnitude difference images without (A) and with (B) motion detection and correction. A clear improvement can be observed indicating that the method is efficient even in the case of non uniform displacements (see Fig. 3).

Fig. 5 compares standard deviation on each pixel for a temporal serie (100 temperature images) before and after correction. All voxels in kidneys and 95% of the voxels in the liver depict an uncertainty lower than 2^oC, satisfying the initial threshold limit.

Fig. 6 illustrates the improvement of the correction technique. Temperature evolution obtained in a single pixel located on the left kidney of the subject (reported on Fig. 1.E) is much more stable (0.8^oC standard deviation) as compared to initial curve (15^oC oscillation amplitude).

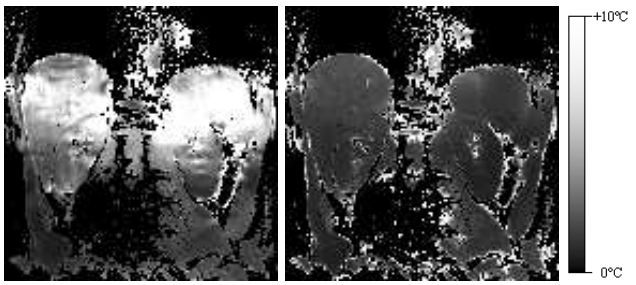

Fig. 5. Temporal standard deviation of the temperature on each pixel of the images before (left) and after (right) correction

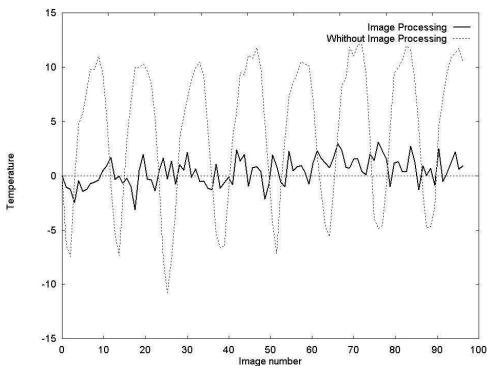

Fig. 6. Temporal evolution of the temperature on the pixel reported on Figure 1.E (white arrow)

5. CONCLUSION

We developed a computational technique that improves temporal resolution of the MR thermometry by a factor of three with respect to the classic technique (respiratory gating). The use of a patient referenced atlas associated with a non rigid transformation model is particularly adapted for motion correction of MR images of the abdomen. Although the computational time per image (250ms) remain compatible with the experimental conditions (400ms), several optimizations have to be implemented. For example, motion registration algorithm could be accelerated (image undersampling, restricted area, ...). Data set contained in the atlas could also be reduced (storing for example mean displacements for each direction) and/or optimized (reduction of the number of positions, and introduction of interpolation techniques). In addition, atlas could also be completed dynamically by introducing data sets corresponding to newly observed positions. This technique opens perspectives towards on line motion tracking for interventional MR-thermometry.

6. REFERENCES

[1] Steiner P., Botnar R., Goldberg S.N., Gazelle G.S., Debatin J.F. Monitoring of radio frequency tissue ablation in an interventional magnetic resonance environment. Preliminary ex-vivo and in-vivo results. Invest. Radio. 1997;32:671-678.

[2] Steiner P., Botnar R., Dubno B. et al. Radio-frequency induced thermoablation: monitoring with T1-weighted and proton frequency shift MR imaging in an interventional 0.5-T environment. Radiology 1998;206:803-810.

[3] Levy S. Biophysical basis and cardiac lesions caused by different techniques of cardiac arrhythmia ablation. Arch. Mal. Coeur Vaiss. 1995;88:1465-1469.

[4] Kim S. Liposomes as carriers of cancer chemotherapy: current status and future prospects. Drugs 1993;46:618-638.

[5] Weinstein J.N., Magin R.L., Yatvin M.B., Zaharko D.S. Liposomes and local hyperthermia: selective delivery of methotrexate to heated tumors. Science 1979;204:188-191.

[6] Madio D.P., van Gelderen P., DesPres D., et al. On the feasibility of MRI-guided focused ultrasound for local induction of gene expression. J. Magn. Res. Imaging 1998;8:101-104.

[7] Mansfield P. et Grannell P.K. NMR "diffraction" in solids?. J. Phys. C:Solid state phys 1973;6,L422-L426.

[8] Quesson B., Jacco A. de Swart, Chrit T.W. Moonen, Magnetic Resonance Temperature Imaging for Guidance of Thermotherapy. Journal of Magnetic Resonance Imaging, 2000;12:523-533.

[9] Denis de Senneville B., Desbarats P., Quesson B., Moonen C. T. W., Real-Time Artefact Corrections For Quantitative MR Temperature Mapping. Journal of WSCG, Vol.11, No.1.,ISSN 1213-6972. WSCG 2003, February 3-7,2003, Plzen, Czech Republic.

[10] Friston K.J., Ashburner J, Frith C.D., Poline J-B., Heather J.D. and Frackowiak R.S.J. Spatial registration and normalisation of images. Human Brain Mapping. 2:165-189. 1995.

[11] Chen M.J. Chen L.G., Chiueh T.D. & Lee Y.P. A new block-matching criterion for motion estimation and its implementation. IEEE Transactions on Circuits and Sytems for Video Technology. 5:231-236. 1995.

[12] Anadan P., "A computational framework and an algorithm for the measurement of visual motion", Intern. J. Comput. Vis. 2:, pp. 283-310, 1989.

[13] Singh A., "An estimation-theoric framework for image-flow computation", Proc. 3rd Itern. Conf. Comput. Vis., Osaka, pp. 168-177, 1990.

[14] Schunck B.G. Horn K.P. - Determining optical flow. *Artificial intelligence*, 17:pp. 185-203,1981.